

Selected Papers

Transition State in a Prevented Proton Transfer Observed in Real Time

Izumi Iwakura,[*1,†,††] **Atsushi Yabushita,**[2] **and Takayoshi Kobayashi**[2,3,4,5]

[1]Innovative use of light and materials/life, PREST, JST, 4-1-8 Honcho, Kawaguchi, Saitama 332-0012

[2]Department of Electrophysics, National Chiao-Tung University, Hsinchu 300, Taiwan

[3]University of Electro-Communications, 1-5-1 Chofugaoka, Chofu, Tokyo 182-8585

[4]ICORP, JST, 4-1-8 Honcho, Kawaguchi, Saitama 332-0012

[5]Institute of Laser Engineering, Osaka University, 2-6 Yamada-oka, Suita, Osaka 565-0971

Received September 17, 2010; E-mail: iwakura@ils.uec.ac.jp

Direct observation of the molecular structural change during chemical reactions including transition states is desirable to fully clarify the mechanism of chemical reactions. Time-dependent frequency variations in *molecular vibration modes* reflect structural change in transition states. Ultrafast changes in molecular structure during bond *breaking* and bond *reformation* can be clearly visualized using ultrafast spectroscopy. This study elucidated molecular structural information in states along the chemical reaction including transition state in the proton transfer of indigodisulfonate salt. The photoexcited proton transfer was found to follow a stepwise pathway. The monoalcohol intermediate generated by the proton transfer was found to return immediately to the original indigo without proton-transfer configuration. This back reaction of this is the reason for the ultra-photostability of indigo over extremely long exposure to light. This shows that real-time vibrational spectroscopy by a few femtosecond pulse laser enables the observation of dynamic behavior of molecular vibrations during chemical reactions, leading to the clarification of reaction mechanisms or the development of new chemical reactions.

The identification of *transition states* (TSs) provides detailed information about reaction mechanisms supplementing information obtained by other means. In the 1990s, several theoretical methods were proposed for inferring the structures of TSs. They were the only methods then available, but their reliability was often questionable. This lack of a robust method prompted chemists to develop an experimental method for visualizing ultrafast changes in molecular structure that proceed via TSs. The experimental realization of femtosecond dynamic studies was developed through the pioneering work of Zewail.[1] More recently, ultrashort pulses[2] whose durations are much shorter than typical molecular vibrational periods have been used to observe structural changes during chemical reactions including TSs.[3] This novel visualization method observes the frequency shifts of the relevant molecular vibration modes. For instance, the photoisomerization dynamics of azobenzene,[3c–3e] bacteriorhodopsin,[3a,3b] and the proton-transfer (PT) reaction[3f–3j] have been elucidated using ultrafast spectroscopy.

Indigo and indigodisulfonate salt are commonly used for dying due to their outstanding photostabilities, which enable them to exist for a long time without undergoing decoloration. Another reason for their common usage is that these dyes are chemically absorbed strongly on cellulose and other fibers. By contrast, several other indigo derivatives, such as perinaphthothioindigo,[4] have relatively high photoisomerization efficiencies (quantum yield: ≈0.25). The photostability of indigo and indigodisulfonate salt were studied in previous works,[5] suggesting the existence of an ultrafast PT reaction in the excited state, which is much faster than photoisomerization. In the present work, the TS in the PT of indigodisulfonate salt was identified by real-time observation of frequency changes and the obtained result was also supported by theoretical analysis. This study experimentally clarifies the riddle of the ultrahigh photostability of indigo and indigodisulfonate salt.

Experimental

Pump–Probe Experiment. A noncollinear optical parametric amplifier (NOPA) was used to obtain an ultra-broadband visible pulse, which was compressed to 5 fs for the ultrafast pump–probe measurement.[2f] A Ti:sapphire regenerative amplifier (Spectra-Physics, model Spitfire, 150 μJ, 100 fs, 5 kHz at 805 nm) was used as a laser source to generate pump and seed pulses of the NOPA. The amplified signal pulse after the double-pass NOPA with a spectrum extending from 525 to 725 nm was compressed with the main compressor, resulting in a pulse duration of 5 fs which is nearly Fourier transform limited (Figure 2b). The experiments were performed at pump and probe pulse intensities of 2580 and 480 GW cm^{-2},

† Present address: Department of Chemistry, Graduate School of Science, Hiroshima University, 1-3-1 Kagamiyama, Higashi-Hiroshima 332-0012

†† Present address: University of Electro-Communications, 1-5-1 Chofugaoka, Chofu, Tokyo 182-8585

Published on the web January 28, 2011; doi:10.1246/bcsj.20100269

respectively. The focal areas of the pump and probe pulse laser were 100 and 75 μm^2, respectively. The polarizations of the pump and the probe pulses are parallel to each other. Sodium indigodisulfonate saturated in anhydrous methanol and methanol-*d*, sodium indigodisulfonate saturated in anhydrous DMSO, and potassium indigodisulfonate saturated in anhydrous methanol in a 1-mm cell were used as samples at 295 ± 1 K. The time-resolved difference transmittance ΔT from 525 to 725 nm was measured simultaneously with a delay time step of 1 fs in the time range of -100 to 800 fs by a 128-channel lock-in amplifier coupled to a polychromator. The spectral resolution of the total system was approximately 1.6 nm.

Computational Methods. The Gaussian 03 program was used for the calculations.[6] Geometric optimizations were performed using the CASSCF/6-31G*//B3LYP/6-311++G**, TD-B3LYP/6-311++G**//B3LYP/6-311++G**, TD-BLYP/6-311++G**//BLYP/6-311++G**, TD-BP86/6-311++G**//BP86/6-311++G**, CIS/6-31++G**//CIS/6-31++G**, and CIS/6-31G*//CIS/6-31G* methods and basis sets. Calculations were performed without assuming symmetry. 5d functions were used for the d orbital. Frequency calculations were performed for all of the obtained structures at the same level, excluding CIS/6-31++G**//CIS/6-31++G**. It was confirmed that all the frequencies were real for the ground states and one imaginary frequency existed for the TS. Vectors of the imaginary frequencies directed the reaction mode and intrinsic reaction coordinate calculations were further performed to confirm that the obtained TSs were on the saddle points of the energy surface between the reactant and the product. However, a concerted pathway could be obtained by the molecular structure optimization only under the condition that the molecule was symmetric with respect to its symmetric center. Theoretical results for the concerted pathway TSs had two imaginary frequencies that were ascribed to $\nu_{s\,N\text{–}H\text{–}O}$ and $\nu_{as\,N\text{–}H\text{–}O}$. When the calculation was performed starting from the calculated results of concerted pathway TSs, which has two imaginary frequencies as initial structures, without symmetry, a more stable TS of the stepwise pathway was obtained.

Spectroscopy. The Ultraviolet/Visible (UV–vis) absorption spectrum of sodium indigodisulfonate methanol solution (3×10^{-6} M) was recorded on an absorption spectrometer (CARY 50, Varian, JAPAN). Emission spectrum of the sample solution (3×10^{-6} M) was recorded on a fluorescence spectrophotometer (FP-6500, JASCO Corp., JAPAN). Both of the measurements were performed using the sample solutions in 1 cm^2 quartz cells at room temperature 293 ± 1 K.

Results and Discussion

Investigation of Reaction Mechanisms of Proton Transfer (Theory). As the PT mechanism of indigo and indigodisulfonate salt after photoexcitation, two possible mechanisms can be considered, i.e., a concerted pathway (two PTs at the same time) or a stepwise pathway (one PT after the other). In order to determine the potential landscape in the two pathways, theoretical analyses were performed using several methods. Figure 1 shows the results calculated by CASSCF/6-31G*//B3LYP/6-311++G**. It represents the calculated results

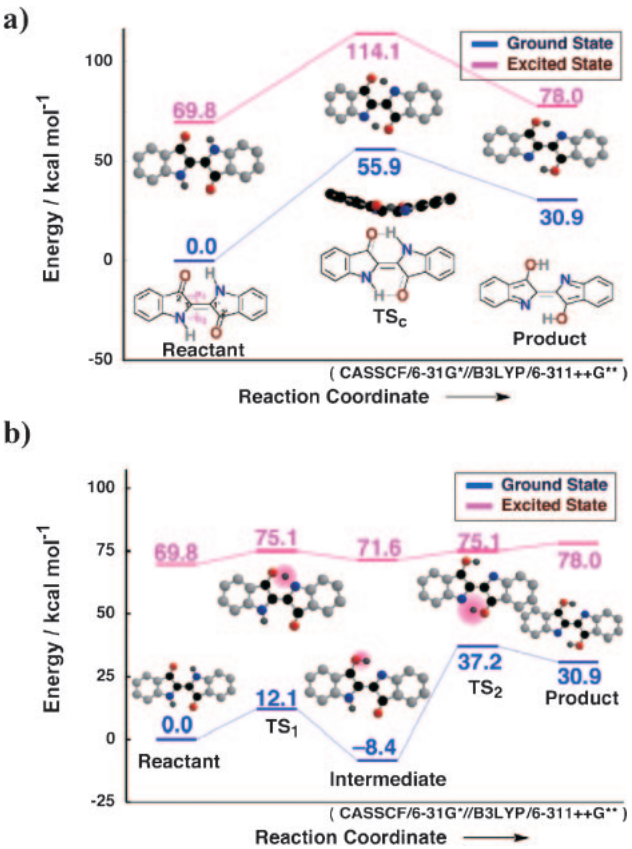

Figure 1. Reaction pathways of the proton transfer in indigo from CASSCF/6-31G*//B3LYP/6-311++G**. a) Concerted pathway. b) Stepwise pathway.

obtained by other methods, which gave essentially the same results (Figure 1, Figures S1–S5 and Table S1 in the Supporting Information (SI)). The calculated activation energy of the concerted pathway in the excited state was larger than 40 kcal mol^{-1} (Figure 1a), ruling out the possibility of a concerted PT. A microscopic mechanism of the concerted pathway can be given as follows. The $C^{1\prime}{=}C^1{-}C^2$ (α_1) and $C^{1\prime}{=}C^1{-}N$ (α_2) bond angles decrease (α_1: 125.8° → 118.7°, α_2: 126.0° → 123.7°) in the TS of the concerted PT (TS_c), as the carbonyl group changes into an alcohol. In the case of the concerted PT mechanism, the change in the bond angle induces deformation of the molecular framework out of the original molecular plane, leading to a bent structure, which dramatically increases the activation energy.

Meanwhile, the stepwise pathway (Figure 1b) is favorable because the activation energy of the TS in the first PT (TS_1) was calculated to be 5.3 kcal mol^{-1}, which is sufficiently low to form the monoalcohol intermediate. However, the second PT is not favorable because the energy surface from the monoalcohol to the product increases gradually.

Therefore, theoretical analysis suggests that the stepwise pathway is energetically more favorable than the concerted pathway. We next investigated these pathways experimentally.

Direct Observation of Transition State (Methanol Solution of Indigodisulfonate Salt). For the direct observation of the dynamics after photoexcitation, 5-fs pump–probe measurement was performed to identify the reaction pathway including

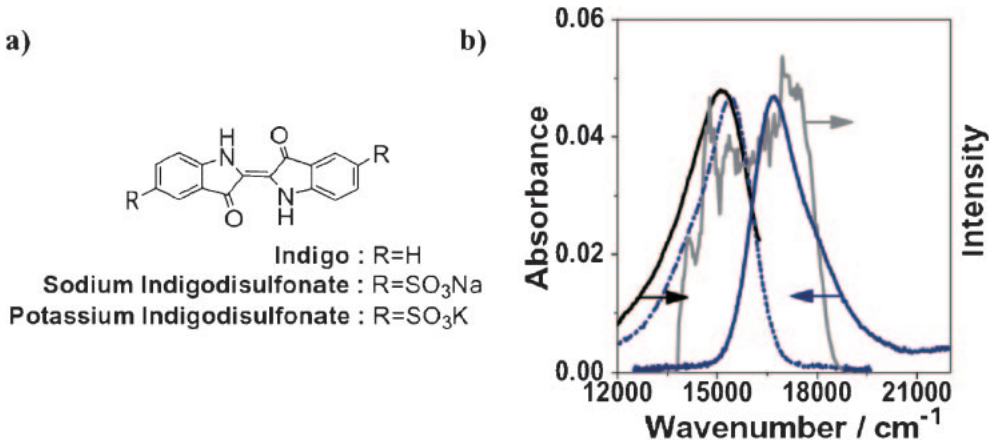

Figure 2. a) Molecular structures of indigo, sodium indigodisulfonate, and potassium indigodisulfonate. b) Absorption (indigo), its mirror image (indigo dots), fluorescence spectrum at 600 nm excitation (black) of sodium indigodisulfonate.[51]

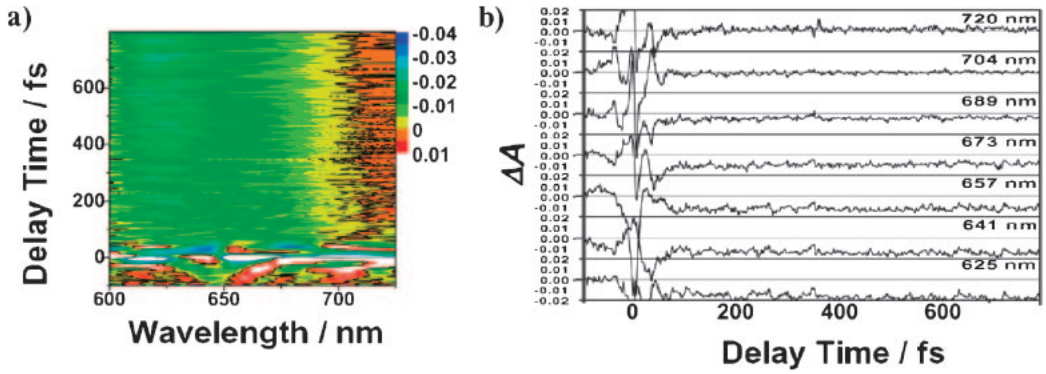

Figure 3. a) A two-dimensional display of the absorbance change on the probe delay time and the wavelength following the 5-fs pulse excitation of the methanol solution of sodium indigodisulfonate.[51] b) Real-time traces of absorbance change.

the TS. A methanol solution of sodium indigodisulfonate, in which photoisomerization does not occur, was used as the sample (Figure 2a). Methanol was used as a solvent, because it has no molecular vibration signal in the frequency range examined. The absorption spectrum of the sample has a peak around 598 nm and the fluorescence spectrum of the sample excited at 600 nm has a peak around 650 nm (Figure 2b). The structure in the excited state is not thought to be rigid because the fluorescence quantum yield is very low (0.0015)[3h] and the fluorescence spectral peak is red shifted from the UV absorption peak (dotted line in Figure 2b).

Figure 3 shows the real-time traces of difference absorbance following the 5-fs pulse excitation of the methanol solution of sodium indigodisulfonate (ΔA, which was calculated as $\Delta A = -\log_{10}(1 + \Delta T/T)$, where T and ΔT are transmittance and transmittance change induced by the pump, respectively) at 128 probe wavelengths. Using a multichannel lock-in amplifier of 128 channels, we observed time-resolved signal over a broad spectral range. The sign for ΔA is positive in the probe wavelength of 715–725 nm due to mainly the induced absorption in the transition from S_1 state to S_n state(s) ($S_n \leftarrow S_1$ transition). Bleaching and stimulated emission still can be observed within the range of 715–725 nm where ΔA is positive, even though their influence becomes smaller at longer wavelengths. The ΔA in the spectral range from 705 to 715 nm oscillates around zero, reflecting the signals of positive ΔA (induced absorption) and negative ΔA (bleaching and stimulated emission). The ΔA in the spectral range $<$705 nm has negative value due to bleaching of the ground-state absorption and stimulated emission of sodium indigodisulfonate. Therefore, dynamics of molecular vibration of excited states can be most sensitively and selectively observed in the spectral range of 715–725 nm. To study the chemical reaction in the excited state, the data in this probe spectral range, 715–725 nm, was used for discussion in this work.

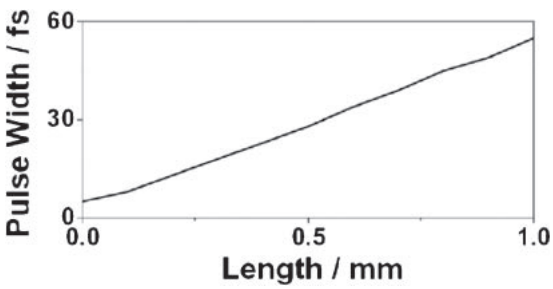

Figure 4. Pulse width after passing through l mm of methanol filled in an optical cell.

From the refractive index of methanol of $n = 1.3195 + 3053.64/\lambda^2 - 3.41636 \times 10^7/\lambda^4 + 2.62128 \times 10^{12}/\lambda^6$ given in Ref. 7, the pulse width after transmission through a 1-mm cell was calculated to be about 55 fs (Figure 4).

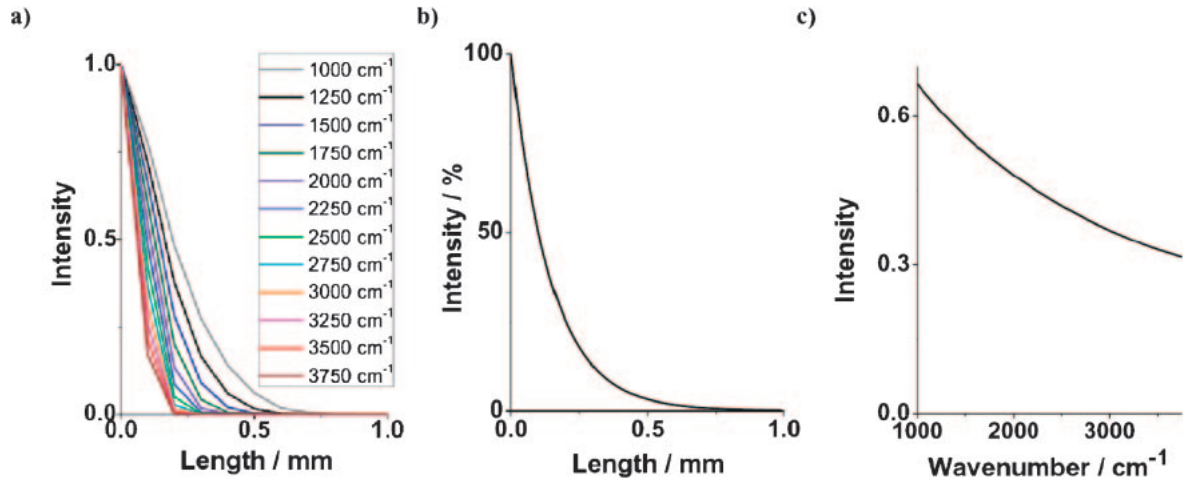

Figure 5. a) Simulation results showing FFT power attenuation for vibration frequencies between 1000 to 3750 cm^{-1} after transmission through a glass cell filled with methanol solution. Different colored curves show the calculation results for 1000 (gray), 1250 (black), 1500 (indigo), 1750 (olive), 2000 (violet), 2250 (blue), 2500 (green), 2750 (cyan), 3000 (orange), 3250 (pink), 3500 (red), and 3750 cm^{-1} (wine). b) Transmission efficiency of photons passing through a glass cell filled with indigo-saturated methanol solution. c) Attenuation ratio of the vibration amplitude whose frequencies are from 1000 to 3750 cm^{-1} after transmission through 1 mm of the indigo-saturated methanol solution.

The pulse width broadening in transmission through the solution cell attenuates the amplitude of molecular vibration observed in the signal as shown in Figure 5a. This paper discusses vibration modes between 1000 and 3750 cm^{-1}. Figure 5b shows the transmission efficiency of photons passing through a glass cell filled with indigo-saturated methanol solution. Figure 5c shows the attenuation ratio of the vibration amplitude for vibration frequencies between 1000 and 3750 cm^{-1} in transmission through the 1-mm glass cell, calculated from Figures 5a and 5b. Their vibration amplitudes cannot be properly resolved by the stretched pulse whose duration is longer than their periods. However, the vibration frequency to be observed is not affected by the stretched pulse width. Hence, their frequency shifts can still be discussed correctly.

Figure 6 shows spectrograms[8] obtained by applying a sliding-window Fourier transform (eq 1).

$$S(\omega,\tau) = \int_0^\infty S(t)g(t-\tau)\exp(-i\omega t)\mathrm{d}t, g(t) = 0.42 - 0.5\cos(2\pi t/T) + 0.08\cos(2\pi t/T) \quad (1)$$

Using a Blackman window function with a full width at half maximum (FWHM) of 120 fs, the spectrogram was calculated from the real-time traces. The frequency resolution of the spectrogram is $\pm 30\ cm^{-1}$. The data near 0 fs could not be analyzed in terms of incoherent electronic transition probabilities proportional to the population modulated by vibration because of the strong interference between the scattered pump and probe pulses.

The spectrogram measured at 720 nm (Figure 6a) shows the smallest influence of bleaching and stimulated emission, since the signal at 720 nm has the largest ΔA compared to the data in the positive ΔA region. Therefore, the spectrogram measured at 720 nm was used as a representative example of excited state dynamics. Similar spectrogram patterns were observed also at probe wavelengths of 715 nm as shown in Figure 6b. Bleaching and stimulated emission still can be observed within the range of 705–725 nm where ΔA is positive, even though their influence becomes smaller at longer wavelengths. Therefore, the spectrogram of 715 nm shows the influence of bleaching and stimulated emission more effectively than that of 720 nm, which gives the spectrogram of 715 nm an osculant shape between that of 720 nm and that of 700 nm.

In the other probe spectral range (<705 nm), both the bleaching and stimulated emission can take part. There is a peak in the absorption spectrum of sodium indigodisulfonate at 598 nm (Figure 2b). Therefore, the ground-state depletion is effective in the spectral range as is also confirmed by the negative sign of ΔA observed. The observed signal in the spectral range shows a C=C stretching vibration mode of the ground state of sodium indigodisulfonate (Figure 6c).

A peak around 1700 cm^{-1}, corresponding to a C=O stretching mode ($\nu_{C=O}$) of reactant (R),[9] appeared just after the excitation. This frequency gradually red-shifted and another peak around 1250 cm^{-1} appeared at 270 fs delay time, which can be attributed to the C–O single bond stretching mode (ν_{C-O}), the frequency of which was reported to be about 1250 cm^{-1}.[5c,10] The presence of this peak indicates the formation of the C–OH group in the intermediate (I). In addition, a spectrogram obtained by methanol solution of potassium indigodisulfonate is similar in the distribution of the Fourier power (Figure 6d).

Comparison between Experimental Results and Theoretical Results TD-B3LYP/6-311++G//B3LYP/6-311++G**.** The observed ultrafast dynamics of the indigodisulfonate salts can be explained by the theoretical results shown in Figure 1 and Table 1. The results of TD-B3LYP/6-311++G**//B3LYP/6-311++G** were used as a representative example. Just after the excitation, two identical C=O groups (R) were observed to give rise to the peak centered around 1700 cm^{-1} (Figure 6), in good agreement with the calculated frequency of 1696 cm^{-1} (Table 1). This peak splits into two red- and blue-shifted peaks in the delay time

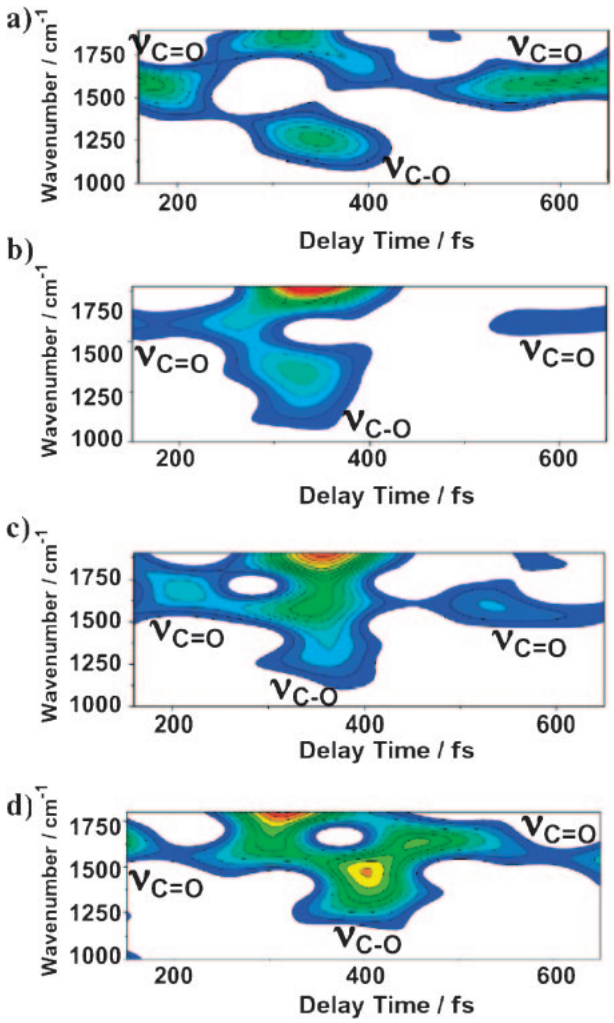

Figure 6. Spectrograms of sodium indigodisulfonate at probe wavelengths of a) 720,[51] b) 715,[51] and c) 700 nm,[51] and d) spectrogram of potassium indigodisulfonate at probe wavelengths of 705 nm.

from 200 to 270 fs. The reason for this frequency shift can be explained as follows. The electron density in one of the two C=O bonds, which is the acceptor of the transferred proton in the first PT, decreases after photoexcitation by π-electron delocalization extending to the transferred proton. This leads to the reduction of $\nu_{C=O}$, which is consistent with the monotonic red shift from 1696 (R) to 1588 cm^{-1} (TS_1) found in the calculated frequencies. On the other hand, the electron density in the C=O bond that does not participate in the first PT is increased after the photoexcitation, which leads to a blue shift of the peak. This is also consistent with the monotonic blue shift of $\nu_{C=O}$ from 1696 (R) to 1751 cm^{-1} (TS_1) in the calculation result. Another possible effect of the shifts of $\nu_{C=O}$ are explained as follows. The indigodisulfonate has a symmetric structure. Therefore, just after the photoexcitation of the indigosulfonate, its structure still keeps symmetry resulting in anharmonic coupling of symmetric and asymmetric $\nu_{C=O}$ modes. The subsequent proton transfer breaks the symmetry reducing the anharmonic coupling between the two C=O bonds, which is also thought to contribute the frequency shift of $\nu_{C=O}$.

The presence of a new peak around 1250 cm^{-1} at 270 fs delay time indicates that the C–OH is formed by the generation of the monoalcohol intermediate, which agrees well with the theoretical results that suggest the appearance of ν_{C-O} (I) at 1276 cm^{-1}. According to the theory, the remaining C=O of the generated monoalcohol is expected to be blue shifted by ca. 70 cm^{-1} [from 1696 (R) to 1763 cm^{-1} (I)], which is in good agreement with the experimentally observed blue shift from 1700 (R) to 1770 cm^{-1} (I). After the generation of the monoalcohol (I), the peak around 1700 cm^{-1} ($\nu_{C=O}$) is reproduced in the time range >500 fs. This is in agreement with the theoretical result that the monoalcohol (I) is energetically unstable compared with the reactant, so that the monoalcohol returns to the reactant rather than forming a product.

The experiments show that the change from C–O to C=O associated with the change from the alcohol to the carbonyl cannot be observed in the back reaction (400–500 fs). One reason for the absence of spectral change is that the vibration dephases due to inhomogeneous and homogeneous broadening. Another reason is that the reaction time of the return path from the alcohol to the carbonyl is too fast to show the change compared with that of the forward path from the carbonyl to the alcohol.

The natural bond orbital (NBO) analysis[11] also supports the experimental observations by showing a second PT does not occur. The bond order of C=O and the distance between **H**–N and **O**=C, which is not responsible for the PT, increase from 1.83 (R) to 1.89 (I) and from 2.28 (R) to 2.42 Å (I), respectively, and the degree of delocalization of π-electrons in C=O bond(s) to the proton is reduced. The NBO analysis also suggests that electron delocalization stabilizes the reactant molecule, but not in the monoalcohol intermediate. In this way, the increase in distance between the H and O atoms supports the experimental results that indicate the first PT takes place, but the second does not.

The transfer of such vibrational coherence or even the creation of coherence by a chemical reaction has been discussed by Jean and Fleming,[12] which explains the weak oscillations clearly observed in the electronic curve crossing. The vibration frequency is too high to be explained by resonant electronic couplings. The high-frequency mode is thought to be a result of coherences between eigenstates with large projections onto diabatic states with different numbers of vibrational quanta. The bare electronic coupling and diabatic vibrational frequency have comparable magnitudes causing considerable interfusion of nonresonant diabatic states. Therefore, the vibrational coherence can be transferred into the product via the electronic curve crossing under sufficiently strong electronic coupling.[13]

These results clearly provide direct evidence that PT takes place after photoexcitation in indigodisulfonate salts and they show that the PT mechanism is a stepwise pathway. The first PT causes the reaction from reactant to intermediate with a high efficiency of >90% estimated from the level of error and noise in the spectrogram, but the generated intermediate also returns to the reactant with high efficiency (>90%). As a result, the total reactivity from reactant to intermediate is negligibly small. Therefore, indigo is very stable and resists discoloration, providing a final answer as to whether or not PT occurs in

Table 1. Theoretical Vibrational Frequencies and NBO Results

		Method:	B3LYP	BLYP	BP86	CIS	CIS	Exp./cm^{-1}
		Basis set:	6-311++G**	6-311++G**	6-311++G**	6-31++G**	6-31G*	
Theoretical results of frequency/cm^{-1}								
Reactant	C=O(1)		1696	1604	1626	—	1855	1700[a)]
	C=O(2)		1696	1604	1626	—	1604	1700[a)]
TS	C=O(1)		1588	1513	1544	—	1513	Red shift
	C=O(2)		1751	1651	1675	—	1651	Blue shift
Intermediate	C–O(1)		1276	1234	1241	—	1234	1250[b)]
	C=O(2)		1763	1656	1678	—	1656	1770[b)]
Bond order								
Reactant	C=O(1)		1.83	1.81	1.81	1.88	1.88	
	C=O(2)		1.83	1.81	1.81	1.88	1.88	
Intermediate	C–O(1)		0.99	0.99	0.99	0.99	0.99	
	C=O(2)		1.89	1.87	1.86	1.91	1.91	
Second-order perturbative estimates of "donor(C=O)–acceptor(H)" interaction in NBO basis/kcal mol^{-1}								
Reactant			8.34	36.79	11.31	7.65	—[c)]	
Intermediate			<0.5	<0.5	<0.5	<0.5	—[c)]	
Distance between C=O and N–H/Å								
Reactant			2.281	2.294	2.264	2.275	2.267	
Intermediate			2.416	2.456	2.483	2.319	2.317	

a) Frequency calculated in the spectrogram at reaction time 100 fs. b) Frequency calculated in the spectrogram at reaction time 360 fs. c) It is thought that the hydrogen bond was not calculated using CIS/6-31G* because there is no diffuse function.

indigo.[3] Direct evidence was obtained indicating that even though PT occurs, the system returns to the original reactant within 0.5 ps. It was concluded that the PT does not take place at the S_1 state on a picosecond scale, and hence indigo is unusually photostable.

Kinetic Isotope Effect (Experiment). For confirmation of the stepwise mechanism in indigodisulfonate salts, the kinetic isotope effect (KIE) was studied by observing the real-time molecular vibration frequency of a deuterated sodium indigodisulfonate (Figure 7a). A peak around 1700 cm^{-1}, corresponding to a C=O stretching mode (R), appeared just after the excitation. This frequency is red-shifted and another peak appeared around 1250 cm^{-1} at ≈450 fs after the photoexcitation in deuterated sodium indigodisulfonate, which is in good agreement with the reported value of C_6H_5OD ($\nu_{C-O} = 1250$ cm^{-1}).[10b]

The reaction rate in deuterated sodium indigodisulfonate was slowed down to $(2.0 \pm 0.1) \times 10^{12}$ s^{-1} from $(3.0 \pm 0.1) \times 10^{12}$ s^{-1} in the non-deuterated system. The primary KIE obtained in the experimental results predicts that the PT rate in the deuteride system was 44% slower than that in the non-deuteride system. The corresponding rate ratio (k_a^H/k_a^D) between H and D ranges widely from 1.15 (in the early TS) to several hundred (in the late TS).

The excited state of sodium indigodisulfonate is expected to have an early TS due to strong hydrogen bonding, and the observed k_a^H/k_a^D ratio was 1.7, which is larger than the expected value (1.15) in the early TS. This is caused by the decrease in k_a^H, indicating that the tunnel effect takes place in the PT of the non-deuterated system. Figure 7a shows that the

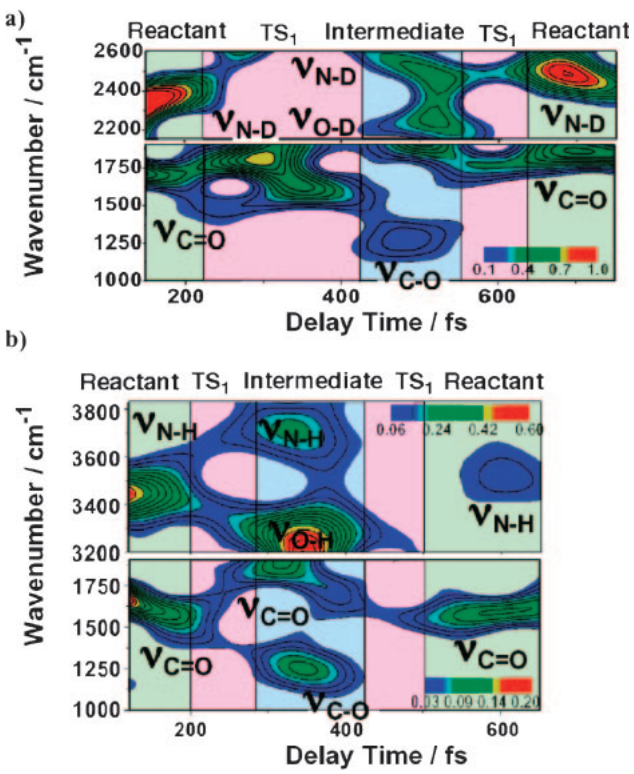

Figure 7. a) Spectrograms of deuterated methanol solution of deuterated sodium indigodisulfonate.[5m] b) Spectrograms of methanol solution of sodium indigodisulfonate.[5l]

frequency of $\nu_{C=O}$ is red shifted from 1700 to about 1500 cm^{-1}, followed by blue shift to about 1600 cm^{-1}, and red shift to about 1250 cm^{-1}. On the other hand, Figure 7b shows that $\nu_{C=O}$ is gradually red-shifted from 1700 to 1250 cm^{-1} without the slow modulation observed in Figure 7a. This slow modulation of the $\nu_{C=O}$ frequency found for the deuterated system is considered to be induced by the coupling of $\nu_{C=O}$ mode with low frequency modes. The low frequency modes can be considered to be scissoring modes of $C^{1'}=C^1-C^2$ (α_1) and $C^{1'}=C^1-N$ (α_2) associated with the deuteron transfer. The mechanism of the mode coupling inducing the modulation can be explained as follows.

In the first deuteron transfer, the distance between N–D and C=O decreases for the deuteron to be transferred to the acceptor. Associated with these processes, the $C^{1'}=C^1-C^2$ bond angle and $C^{1'}=C^1-N$ bond angle are expected to decrease and increase, respectively, with decrease in the carbon–carbon bond order changing from carbon–carbon double bond to carbon–carbon single bond. These bond angle changes in turn trigger the scissoring modes of $C^{1'}=C^1-C^2$ and $C^{1'}=C^1-N$. On the other hand, the oscillatory feature of $\nu_{C=O}$ was not found in the non-deuterated sample. It is thought to be due to much faster proton-transfer rate than the scissoring period.

In addition, in the spectrogram of sodium indigodisulfonate, a peak around 3350 cm^{-1} appeared just after the excitation and was assigned to the N–H stretching mode (ν_{N-H}) (Figure 7b). The frequency of the peak displayed a gradual red shift and another peak around 3185 cm^{-1} appeared at ca. 270 fs after the photoexcitation. The peak located at 3185 cm^{-1} was attributed to the O–H stretching mode (ν_{O-H}), because the new peak appeared at almost the same time as that for ν_{C-O}. The red shift was thought to be due to PT-induced generation of the monoalcohol (I), which has an O–H instead of N–H. The vibrational frequency of the latter (3185 cm^{-1}) is lower than the former (3350 cm^{-1}) by about $(14/16)^{1/2}$. On the other hand, the electron density in the other N–H bond, which does not participate in the PT, is increased during the PT, leading to the blue-shift of the peak, because hydrogen bonding is weakened during the PT. When the generation of the monoalcohol (I) is complete, the peak around 3350 cm^{-1} (ν_{N-H}) is reproduced, as shown at the later delay time (>500 fs) in Figure 7b.

In the spectrogram of deuterated sodium indigodisulfonate, a peak appeared around 2380 cm^{-1} just after the photoexcitation and was assigned to a N–D stretching mode (ν_{N-D}) (Figure 7a). This frequency is lower than that of non-deuterated sodium indigodisulfonate by a factor of $(2)^{-1/2}$. This mode frequency also showed a gradual red-shift and another peak appeared around 2200 cm^{-1} at ca. 500 fs delay time. The peak located at 2200 cm^{-1} is thought to be due to the O–D stretching mode (ν_{O-D}), because the new peak appeared at the same time as ν_{C-O}. The reason for the lowering of the frequency from 2380 to 2200 cm^{-1} is that the PT during the generation of the monoalcohol (I) changes N–D to O–D, causing the red shift of the molecular vibration frequency by a factor of $(14/16)^{1/2}$. Meanwhile, the electron density in the other N–H bond, which does not participate in the PT, is increased after the photo-excitation, leading to the blue shift of the peak due to the weakened hydrogen bonding. After the generation of monoalcohol (I), the peak around 2380 cm^{-1} (ν_{N-D}) was restored in the longer delay time region of >700 fs, as shown in Figure 7a. These results are completely consistent with that for the carbonyl group dynamics.

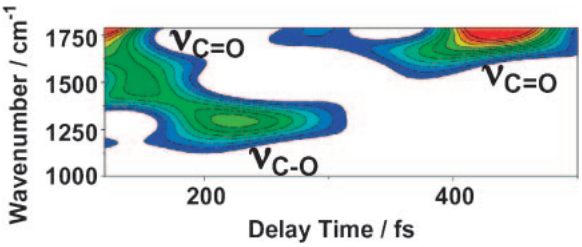

Figure 8. Spectrogram of DMSO solution of sodium indigodisulfonate.

The small delay between the appearance of the ν_{O-H} and ν_{C-O} seen in Figure 7 can be explained as follows. The theoretical calculation shows that the distance between C=**O** and N–**H** decreases considerably in generating the O–H bond, from 2.279 Å in the reactant to almost half of that in the TS (1.197 Å), and even shorter in the intermediate (0.986 Å). However, the C=O bond length changes only slightly from the reactant (1.236 Å) to the TS (1.296 Å) and the intermediate (1.334 Å), to generate the C–O bond. Therefore, the appearance of ν_{C-O} is delayed slightly compared with that of ν_{O-H}.

Solvent Effect. As mentioned above, in the case of methanol solution of indigodisulfonates salts, ultrafast PT in the excited state takes place by the stepwise mechanism. However, whether the PT takes place intramolecularly or intermolecularly is not understood, because the methanol is a protic solvent. Therefore, the DMSO solution, which is aprotic solvent, of sodium indigodisulfonate was used as a sample. The obtained spectrogram is shown in Figure 8. In the spectrogram, a peak around 1700 cm^{-1}, due to a C=O stretching mode of reactant, appeared just after the excitation. This frequency gradually red-shift in time toward 200 fs, and other peaks around 1250 and 1750 cm^{-1} started to appear. The peak around 1250 cm^{-1} can be attributed to the C–O single bond stretching mode (ν_{C-O}). The presence of this peak indicates the formation of the C–OH group in the intermediate. After the generation of the monoalcohol (I), the peak around 1700 cm^{-1} ($\nu_{C=O}$) is reproduced in the time range >350 fs. If the PT takes place by intramolecular reaction in the methanol solution, the reaction time of the PT in methanol solution is close to that in the DMSO solution. These results show that the reaction time scales are almost the same between the DMSO solution and the methanol solution, but the reaction time of the PT in the DMSO solution is a little faster than that in the methanol solution. Therefore, the possibility of intramolecular PT reaction in the methanol solution is high. However, the possibility of intermolecular PT reaction in the methanol solution cannot be denied. Anyway, these results confirm that PT takes place after photoexcitation in indigodisulfonate salts in both protic and aprotic solvents, and they show that the PT mechanism is a stepwise pathway. Moreover, the unstable monoalcohol (I) generated by PT then reverts to the reactant indigo compound.

Conclusion

In summary, the structural change during ultrafast proton transfer via a transition state was observed using an ultrashort

pulse laser. It was concluded that a photoexcited proton transfer takes place in indigodisulfonate salts by the stepwise mechanism. To date, the reason why indigo is photostable could not be elucidated for over 100 years. The answer was obtained by the direct experimental observation in this work. The efficiency of photodiscoloration of indigodisulfonate salts caused by photoisomerization is suppressed by a single proton transfer after photoexcitation, because the molecular structure was fixed in the planar form by the formation of a monoalcohol intermediate generated by the single proton transfer. The unstable monoalcohol intermediate generated by the proton transfer then reverts to the reactant indigo compound. Thus, time-resolved spectroscopy with time resolution of a few femtoseconds provides a new way to clarify mechanisms and stimulate novel ideas for the development of new chemical reactions. Clarification of detailed reaction mechanisms is enabled by application of this technique to the study of ultrafast dynamics in various fields, such as photochemistry, photophysics, and photobiology.

The authors thank Dr. Takashi Hirano of Univ. of Electro-Communications for his help in the measurement of stationary fluorescence and absorption spectra of the sample. The authors are grateful to the Information Technology Centre of the University of Electro-Communications for their support of the computational calculations.

Supporting Information

The energies of the most stable conformers and energy profiles of various methods. This material is available free of charge on the Web at: http://www.csj.jp/journals/bcsj/.

References

1 A. H. Zewail, *J. Phys. Chem. A* **2000**, *104*, 5660.

2 a) P. C. Becker, R. L. Fork, C. H. B. Cruz, J. P. Gordon, C. V. Shank, *Phys. Rev. Lett.* **1988**, *60*, 2462. b) A. Stingl, Ch. Spielmann, F. Krausz, R. Szipöcs, *Opt. Lett.* **1994**, *19*, 204. c) J. Zhou, C.-P. Huang, C. Shi, M. M. Murnane, H. C. Kapteyn, *Opt. Lett.* **1994**, *19*, 126. d) A. Baltuska, Z. Wei, M. S. Pshenichnikov, D. A. Wiersma, *Opt. Lett.* **1997**, *22*, 102. e) M. Nisoli, S. De Silvestri, O. Svelto, R. Szipöcs, K. Ferencz, Ch. Spielmann, S. Sartania, F. Krausz, *Opt. Lett.* **1997**, *22*, 522. f) A. Baltuška, T. Fuji, T. Kobayashi, *Opt. Lett.* **2002**, *27*, 306.

3 a) R. A. Mathies, C. H. B. Cruz, W. T. Pollard, C. V. Shank, *Science* **1988**, *240*, 777. b) T. Kobayashi, T. Saito, H. Ohtani, *Nature* **2001**, *414*, 531. c) T. Saito, T. Kobayashi, *J. Phys. Chem. A* **2002**, *106*, 9436. d) T. Fujino, S. Y. Arzhantsev, T. Tahara, *Bull. Chem. Soc. Jpn.* **2002**, *75*, 1031. e) J. Bredenbeck, J. Helbing, A. Sieg, T. Schrader, W. Zinth, C. Renner, R. Behrendt, L. Moroder, J. Wachtveitl, P. Hamm, *Proc. Natl. Acad. Sci. U.S.A.* **2003**, *100*, 6452. f) A. Mühlpfordt, U. Even, N. P. Ernsting, *Chem. Phys. Lett.* **1996**, *263*, 178. g) C. Chudoba, E. Riedle, M. Pfeiffer, T. Elsaesser, *Chem. Phys. Lett.* **1996**, *263*, 622. h) S. Lochbrunner, A. J. Wurzer, E. Riedle, *J. Chem. Phys.* **2000**, *112*, 10699. i) M. Rini, A. Kummrow, J. Dreyer, E. T. J. Nibbering, T. Elsaesser, *Faraday Discuss.* **2003**, *122*, 27. j) M. Rini, J. Dreyer, E. T. J. Nibbering, T. Elsaesser, *Chem. Phys. Lett.* **2003**, *374*, 13. k) S. J. Schmidtke, D. F. Underwood, D. A. Blank, *J. Am. Chem. Soc.* **2004**, *126*, 8620.

4 C. P. Klages, K. Kobs, R. Memming, *Chem. Phys. Lett.* **1982**, *90*, 51.

5 a) W. R. Brode, E. G. Pearson, G. M. Wyman, *J. Am. Chem. Soc.* **1954**, *76*, 1034. b) J. Weinstein, G. M. Wyman, *J. Am. Chem. Soc.* **1956**, *78*, 2387. c) W. Lüttke, M. Klessinger, *Chem. Ber.* **1964**, *97*, 2342. d) M. Klessinger, W. Lüttke, *Chem. Ber.* **1966**, *99*, 2136. e) G. M. Wyman, *J. Chem. Soc. D* **1971**, 1332. f) T. Kobayashi, P. M. Rentzepis, *J. Chem. Phys.* **1979**, *70*, 886. g) T. Elsaesser, W. Kaiser, W. Lüttke, *J. Phys. Chem.* **1986**, *90*, 2901. h) J. Seixas de Melo, A. P. Moura, M. J. Melo, *J. Phys. Chem. A* **2004**, *108*, 6975. i) Y. Nagasawa, R. Taguri, H. Matsuda, M. Murakami, M. Ohama, T. Okada, H. Miyasaka, *Phys. Chem. Chem. Phys.* **2004**, *6*, 5370. j) J. Sérgio Seixas de Melo, R. Rondão, H. D. Burrows, M. J. Melo, S. Navaratnam, R. Edge, G. Voss, *ChemPhysChem* **2006**, *7*, 2303. k) A. Doménech, M. T. Doménech-Carbó, M. L. Vázquez de Agredos Pascual, *J. Solid State Electrochem.* **2007**, *11*, 1335. l) I. Iwakura, A. Yabushita, T. Kobayashi, *Chem. Lett.* **2009**, *38*, 1020. m) I. Iwakura, A. Yabushita, T. Kobayashi, *Chem. Phys. Lett.* **2010**, *484*, 354.

6 M. J. Frisch, G. W. Trucks, H. B. Schlegel, G. E. Scuseria, M. A. Robb, J. R. Cheeseman, J. A. Montgomery, Jr., T. Vreven, K. N. Kudin, J. C. Burant, J. M. Millam, S. S. Iyengar, J. Tomasi, V. Barone, B. Mennucci, M. Cossi, G. Scalmani, N. Rega, G. A. Petersson, H. Nakatsuji, M. Hada, M. Ehara, K. Toyota, R. Fukuda, J. Hasegawa, M. Ishida, T. Nakajima, Y. Honda, O. Kitao, H. Nakai, M. Klene, X. Li, J. E. Knox, H. P. Hratchian, J. B. Cross, V. Bakken, C. Adamo, J. Jaramillo, R. Gomperts, R. E. Stratmann, O. Yazyev, A. J. Austin, R. Cammi, C. Pomelli, J. W. Ochterski, P. Y. Ayala, K. Morokuma, G. A. Voth, P. Salvador, J. J. Dannenberg, V. G. Zakrzewski, S. Dapprich, A. D. Daniels, M. C. Strain, O. Farkas, D. K. Malick, A. D. Rabuck, K. Raghavachari, J. B. Foresman, J. V. Ortiz, Q. Cui, A. G. Baboul, S. Clifford, J. Cioslowski, B. B. Stefanov, G. Liu, A. Liashenko, P. Piskorz, I. Komaromi, R. L. Martin, D. J. Fox, T. Keith, M. A. Al-Laham, C. Y. Peng, A. Nanayakkara, M. Challacombe, P. M. W. Gill, B. Johnson, W. Chen, M. W. Wong, C. Gonzalez, J. A. Pople, *Gaussian 03, Revision D.02*, Gaussian, Inc., Wallingford CT, **2004**.

7 I. Z. Kozma, P. Krok, E. Riedle, *J. Opt. Soc. Am. B* **2005**, *22*, 1479.

8 M. J. J. Vrakking, D. M. Villeneuve, A. Stolow, *Phys. Rev. A* **1996**, *54*, R37.

9 a) T. M. Ivanova, G. M. Ostapchuk, L. B. Shagalov, V. N. Berdyugin, *Khim. Geterotsikl. Soedin.* **1981**, 501. b) I. T. Shadi, B. Z. Chowdhry, M. J. Snowden, R. Withnall, *Chem. Commun.* **2004**, 1436. c) R. Giustetto, F. X. Llabrés i Xamena, G. Ricchiardi, S. Bordiga, A. Damin, R. Gobetto, M. R. Chierotti, *J. Phys. Chem. B* **2005**, *109*, 19360.

10 a) R. L. Hinman, *J. Org. Chem.* **1964**, *29*, 1449. b) G. Keresztury, F. Billes, M. Kubinyi, T. Sundius, *J. Phys. Chem. A* **1998**, *102*, 1371.

11 E. D. Glendening, A. E. Reed, J. E. Carpenter, F. Weinhold, *Gaussian NBO, Version 3.1*.

12 J. M. Jean, G. R. Fleming, *J. Chem. Phys.* **1995**, *103*, 2092.

13 a) F. Rosca, A. T. N. Kumar, X. Ye, T. Sjodin, A. A. Demidov, P. M. Champion, *J. Phys. Chem. A* **2000**, *104*, 4280. b) A. T. N. Kumar, F. Rosca, A. Widom, P. M. Champion, *J. Chem. Phys.* **2001**, *114*, 701.